

## **Electrorheological Fluid Based Force Feedback Device**

Charles Pfeiffer<sup>a</sup>, Constantinos Mavroidis<sup>a</sup>, Yoseph Bar-Cohen<sup>b</sup>, Benjamin Dolgin<sup>b</sup>

<sup>a</sup>Department of Mechanical and Aerospace Engineering, Rutgers University,  
The State University of New Jersey, 98 Brett Rd., Piscataway, NJ 08854-8058

<sup>b</sup>Jet Propulsion Laboratory, California Institute of Technology,  
4800 Oak Grove Drive, Pasadena, CA 91109-8099

### **ABSTRACT**

Force feedback from remote or virtual operations is needed for numerous technologies including robotics, tele-presence, teleoperation (e.g., surgery, etc.), games and movies. To address this need, the authors are investigating the use of electrorheological fluids (ERF) for their property to change the viscosity under electrical stimulation. This property offers the capability to produce feedback haptic devices that can be controlled in response to remote or virtual stiffness conditions. Forces applied at a robot end-effector due to a compliant environment can be reflected to the user using such an ERF device where a change in the system viscosity in proportion to the force to be transmitted. This paper describes the analytical modeling and experiments that are currently underway to develop an ERF based force feedback element.

**Keywords:** Haptic Interfaces, Telepresence, Robots as Human Surrogate, Electroactive Polymers, Electrorheological Fluids.

## **1. INTRODUCTION**

### **1.1 Telepresence**

For many years, the robotic community sought to develop robots that can eventually operate autonomously and eliminate the need for human operators. However, there is an increasing realization that there are some tasks that humans can perform significantly better but, due to associated hazards, distance, physical limitations and other causes, only robots can be employed to perform these tasks. Remotely performing these tasks by operating robots as human surrogates is referred to as telepresence. In telepresence the operator receives sufficient information about the remote robot and the task environment displayed in a sufficiently natural way, that the operator would be able to feel the equivalent of physical presence at the remote site [1]. Haptic feedback is necessary for a telepresence system where physical constraints such as object rigidity, mass and weight, friction, dynamics, surface characteristics (smoothness or temperature) are mirrored to the human operator from the remote site [2, 3]. An example of a force-feedback telepresence system is schematically shown in Figure 1.

Outer space and extraterrestrial bodies are good examples of environments where telepresence control of surrogate robots is needed. As human activity in space increases, there is an increasing need for robots to perform dexterous extra-vehicular activities (EVA) tasks. Existing space robots such as the Space Station Remote Manipulator System (SSRMS) and the Special Purpose Dexterous Manipulator (SPDM) are inadequate substitutes for an astronaut because they require additional special alignment targets and grapple fixtures, and they are too large to fit through tight EVA access corridors. These robots do not possess adequate speed and dexterity to handle small and complex items, soft and flexible materials, or most common EVA interfaces. Therefore, there is a great need for dexterous, fast, accurate, teleoperated space robots that provide the operator the ability to "feel" the environment as if she or he is "present" at the robot's operation field.

---

Correspondence: C. Mavroidis. Other author information: C.P.; Email: cpfeiffe@caip.rutgers.edu; Telephone: 732-445-2322; Fax: 732-445-3124. C.M.; Email: mavro@jove.rutgers.edu; Telephone: 732-445-0732; Fax: 732-445-3124. Y.B.; Email: yosi@jpl.nasa.gov; Telephone: 818-354-2610; Fax: 818-393-4057. B.D.; Email: Benjamin.P.Dolgin@jpl.nasa.gov; Telephone: 818 354-5017; Fax: 818 393-4057.

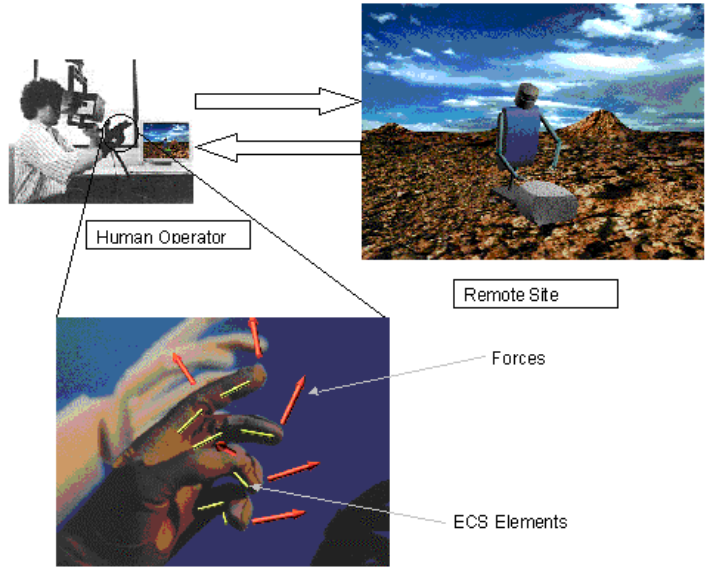


**Figure 1.** Performing Remote Tasks via a Haptic Interface

## 1.2 Robonaut

Robots capability to operate as a surrogate human, which includes telepresence and performance of remote missions, has been recently implemented at NASA Johnson Space Center (see Figures 2, 3 and 4) with the development of the novel space robot called Robonaut (see Figure 2). This robot is capable of performing various tasks at remote sites [4] and serve as a robotic astronaut on the International Space Station, providing a relatively fast response time and the ability to maneuver through areas too small for the current Space Station robots. Robonaut is developed to support high-payoff EVA tasks and to provide "minuteman"-like responses to EVA contingencies. The Robonaut is designed as an anthropomorphic robot, similar in size to a suited EVA astronaut and as a telepresence system that immerses the remote operator into the robot's environment. The robotic arms are capable of dexterous, human-like maneuvers and are designed to ensure safety and mission success. The robotic hands are designed to handle common EVA tools, to grasp irregularly shaped objects, and to handle a wide spectrum of tasks requiring human-like dexterity (Figure 3). For stabilization, the "stinger-tail" of Robonaut will be plugged into the worksite interface (WIF) sockets conveniently located around the ISS. The Robonaut potentially can be carried by the crew equipment translation aid (CETA) to various EVA worksites, or can be picked up by the SSRMS for "end-of-arm" tasks (Figure 4) [4, 5].



**Figure 2.** Robonaut

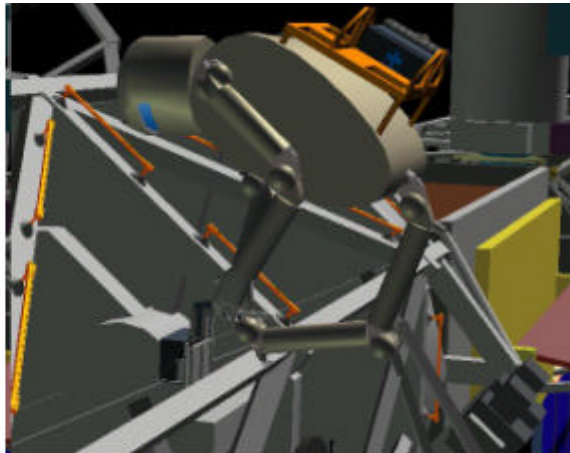


**Figure 3.** Robonaut Performing Repair Work



**Figure 4:** Robonaut Secured to Mount

Figures 2-4 are showing a simulation.

Robonaut was designed so that a human operator who is wearing gloves/suit with sensors can control it. In the case of the Robonaut project, the human operator must control nearly fifty individual degrees of freedom. Using three axis hand

controllers would present a formidable task for the operator. Because Robonaut is anthropomorphic, the logical method of control is one of a master-slave relationship whereby the operator's motions are essentially mimicked by the robot. If the user is to interact in a natural way with the robot, the interface must be intuitive, accurate, responsive, transparent and reproducible over time and space. If the user is to control the robot motions in a naturally perceived way, an interface device must be provided which is capable of determining what the user is doing without interfering with his/her motion or encumbering his/her body. Furthermore, the operator must be able to extract information about the robot and its environment to effectively control the robot. Unfortunately, due to unavailability of force and tactile feedback capability in the control suit/glove, the operator determines the required action by visual feedback, i.e. looking at the Robonaut action at the remote site. This approach is ineffective and is limiting the potential tasks that Robonaut can perform. This hampers the successful completion of delicate or dexterous tasks.

### **1.3 Haptic Interfaces - Background**

At the present time, haptic feedback is less developed than either visual or auditory feedback. Tactile feedback is easier to produce than force feedback with present actuator technology, and the interface tends to be light and portable. An example is the tactile feedback suit that was developed by Begej Co. for NASA JSC [6]. While tactile feedback was conveyed by the mechanical smoothness and slippage of a remote object, it could not produce rigidity of motion [7]. Thus, tactile feedback alone cannot convey the mechanical compliance, weight or inertia of the virtual object being manipulated.

Non-portable devices, such as force feedback joysticks, mice [8, 9, 10] and small robotic arms such as the Phantom [11, 12] allow users to feel the geometry, hardness and/or weight of virtual objects without tiring the user. A desk supports the interface. But this support inherently limits the freedom of motion and dexterity. Portable systems, such as "Force ArmMaster" produced by EXOS Co. under a NASA SBIR task, allow users to move their hand freely, but are often heavy and cause fatigue after extended use.

Luecke and his colleagues at Iowa State University did work towards improved master portability with more freedom of motion [13]. Their haptic interface consists of an exoskeleton hand master tracked and supported by a robot. Similar work was done at NASA Jet Propulsion Laboratory (JPL). The scientists retrofitted an older JPL Universal Master [14] producing wrist force feedback with a 16 degree-of-freedom hand master [15]. The master- structure weighs about 2.5-lb and can move within a 30x30x30-cm cube.

Burdea and his colleagues at Rutgers University proposed a light force feedback hand master designed to retrofit open-loop sensing gloves [16, 17]. The Rutgers RMII has low-friction custom graphite-glass actuators, which output up to 16 N/fingertip with very high dynamic range. However, the palm can not close completely so that it is not possible to feel remote/virtual objects with small dimensions.

The CyberGrasp is another lightweight, force-reflecting exoskeleton glove that fits over a CyberGlove and adds resistive force feedback to each finger via a network of tendons routed around an exoskeleton [18]. The actuators are high-quality DC motors located in a small enclosure on the desktop. The remote reaction forces can be emulated very well; however, it is difficult to reproduce the feeling of "remote stiffness". Also, the operator is "attached" to the desktop with the cable network, limiting portability.

To date, there are no effective commercial unencumbering haptic feedback devices for the human hand. Current "hand master" haptic systems, while they are able to reproduce the feeling of rigid objects, present great difficulties to emulate the feeling of remote/virtual stiffness. In addition, they tend to be heavy, cumbersome and usually they only allow limited operator workspace.

### **1.4 Remote MEchanical MIRroring using Controlled stiffness and Actuators (MEMICA)**

This paper presents the development of haptic interfacing mechanism that will enable a remote operator to "feel" the stiffness and forces at remote or virtual sites. These interfaces will be based on novel mechanisms that were conceived by JPL and Rutgers University investigators, in a system called MEMICA [19, 20]. The key aspect of the MEMICA system is a miniature electrically controlled stiffness (ECS) element that mirrors the stiffness at remote/virtual sites. The ECS elements make use of electro-rheological fluid (ERF), which is an electroactive polymer (EAP), to achieve this feeling of stiffness. The ECS elements will be placed at selected locations on an instrumented glove to mirror the forces of resistance to motion at the corresponding locations at the robot hand. Forces applied at the robot end-effector due to a compliant environment will be reflected to the user using this ERF device where a change in the system viscosity will occur proportionally to the force to be transmitted. A schematic of the MEMICA concept is shown in Figure 1. The MEMICA system consists also of force feedback actuation tendon (FEAT) elements, which employ other type of actuators to mirror forces induced by active elements at the remote or virtual site. The description of FEAT elements is outside the scope of this paper.

## 2. SYSTEM OVERVIEW

### 2.1 Electro-Rheological Fluids (ERFs)

Electro-rheological fluids (ERFs) are fluids that experience dramatic changes in rheological properties, such as viscosity, in the presence of an electric field. Willis M. Winslow first explained the effect in the 1940s using oil dispersions of fine powders [21]. The fluids are made from suspensions of an insulating base fluid and particles on the order of one tenth to one hundred microns in size. The electro-rheological effect, sometimes called the *Winslow effect*, is thought to arise from the difference in the dielectric constants of the fluid and particles. In the presence of an electric field, the particles, due to an induced dipole moment, will form chains along the field lines (Figure 5). This induced structure changes the ERF's viscosity, yield stress, and other properties, allowing the ERF to change consistency from that of a liquid to something that is viscoelastic, such as a gel, with response times to changes in electric fields on the order of milliseconds. A good review of the ERF phenomenon and the theoretical basis for their behavior can be found in [22, 23].

Control over a fluid's rheological properties offers the promise of many possibilities in engineering for actuation and control of mechanical motion. Devices that rely on hydraulics can benefit from ERF's quick response times and reduction in device complexity. Their solid-like properties in the presence of a field can be used to transmit forces over a large range and have found a large number of applications [24]. Devices designed to utilize ERFs include shock absorbers, active dampers, clutches, adaptive gripping devices, and variable flow pumps [25, 26]. An engineering application of ERFs is vibration control and a good review of the subject can be found in [27]. The application of ERFs in robotic and haptic systems has been very limited. They have mainly been used as active dampers for vibration suppression [28].

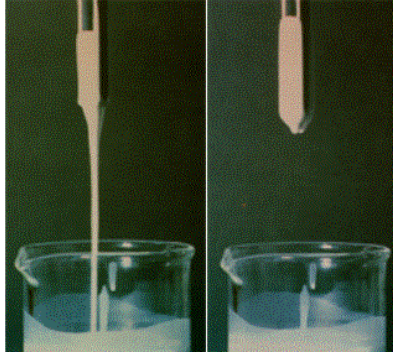


**Figure 5.** Electro-Rheological Fluid at Reference (left) and Activated States (right)

ERFs are generally recognized as behaving according to the Bingham plastic model for fluid flows, meaning that they will behave as a solid up to a certain yield stress. At stresses higher than this yield stress, the fluid will flow, and the shear stress will continue to increase with the shear rate, so that:

$$\mathbf{t} = \mathbf{t}_y + \mathbf{m}\dot{\mathbf{g}} \quad (1)$$

where:  $\mathbf{t}$  is the shear stress,  $\mathbf{t}_y$  is the yield stress,  $\mathbf{m}$  is the dynamic viscosity and  $\dot{\mathbf{g}}$  is the shear strain. The dot over the shear strain indicates its time derivative, the shear rate. In general, both the yield stress and the viscosity will be functions of the electric field strength.

In this work, the electro-rheological fluid LID 3354, manufactured by ER Fluid Developments Ltd., has been used [29]. LID 3354 is an electro-rheological fluid made up of 35% by volume of polymer particles in fluorosilicone base oil. It is designed for use as a general-purpose ER fluid with an optimal balance of critical properties and good engineering behavior. Solid and liquid are density matched to minimize settling. LID 3354 can be used in suitable equipment wherever electronic control of mechanical properties is required, such as in controlled dampers, actuators, clutches, brakes and valves. Its physical properties are: density:  $1.46 \times 10^3 \text{ kg/m}^3$ ; viscosity: 125 mPa.sec at 30°C; boiling point: > 200°C; flash point: >150°C; insoluble in water; freezing point: < -20°C.

The field dependencies for this particular ERF are:

$$\mathbf{t}_{y,s} = C_s (E - E_{ref}) \quad \mathbf{t}_{y,d} = C_d E^2 \quad \mathbf{m} = \mathbf{m}_o - C_v E^2 \quad (2)$$

where:  $m$ , is the zero field viscosity;  $C_s$ ,  $C_d$ ,  $C_v$  and  $E_{ref}$  are constants supplied by the manufacturer. The subscripts s and d correspond to the static and dynamic yield stresses. The formula for static yield stress is only valid for fields greater than  $E_{ref}$ . Figures 6a, b, and c are a graphical representation of Equations (2) for the ERF LID 3354. Figure 6d shows the dependency of the current density at 30°C as a function of the field. Figure 6e shows the coefficient  $C_d$  of Equation (2) as a function of the temperature.

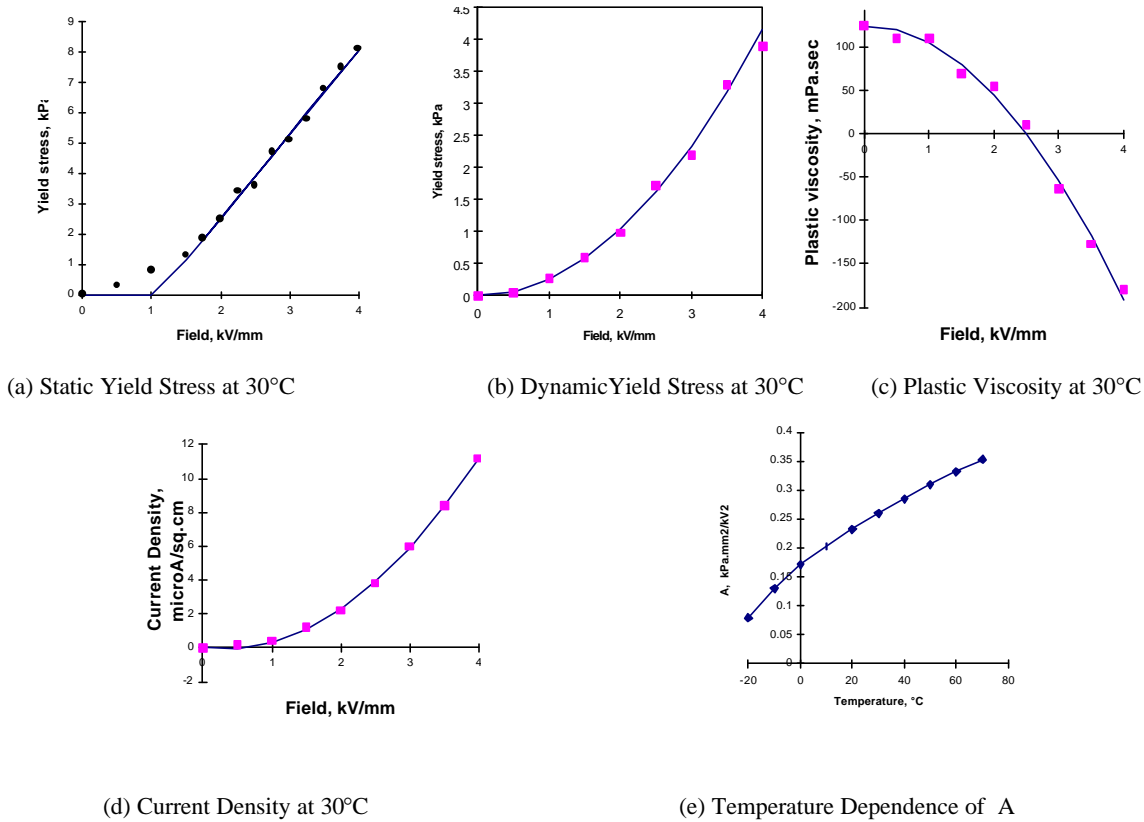


**Figure 6.** Technical Information Diagrams for the ER Fluid LID 3354

## 2.2 MEMICA and ECS Elements

As mentioned earlier, MEMICA is a haptic interface system that consists of a glove equipped with a series of electrically controlled stiffness (ECS) elements as it is schematically shown in Figure 1. Each finger needs to be equipped with one or more of these elements to maximize the level of stiffness/force feedback that is "felt" by the operator as he/she applies activation pressure.

Miniature electrically controlled stiffness (ECS) elements are responsible for mirroring the level of mechanical resistance to the applied forces by the remote or virtual robots at specific joints/points. The element stiffness is modified electrically by controlling the flow of an electro-rheological fluid (ERF) through slots on the side of or embedded in the piston (Figure 7). The ECS element consists of a piston that is designed to move inside a sealed cylinder filled with ERF. The rate of flow is controlled electrically by electrodes facing the flowing ERF while inside the channel.

To control the "stiffness" of the ECS, a voltage is applied between electrodes that are facing the slot and the ability of the liquid to flow is affected. Thus, the slot serves as a liquid valve since the increased viscosity decreases the flow rate of the ERF and varies the stiffness that is felt. To increase the stiffness bandwidth, ranging from free flow to maximum viscosity, multiple slots are made along the piston surface. To wire such a piston to a power source, the piston and its shaft are made hollow and electric wires are connected to electrode plates mounted on the side of the slots. The inside surface of the ECS cylinder surrounding the piston is made of a metallic surface and serves as the ground and opposite polarity. A sleeve covers the piston shaft to protect it from dust, jamming or obstruction. When a voltage is applied, potential is developed through the ERF that flows along the piston channels and its viscosity is altered. As a result of the increase in the ERF viscosity, the flow is slowed significantly and increases the resistance to external axial forces.

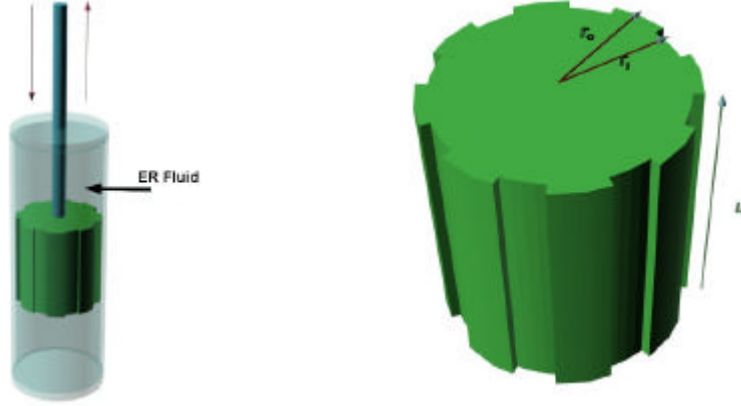


**Figure 7.** ECS Element and Close-Up View of the Piston

### 3. MODELING OF ECS ELEMENT

In order to optimally design and control the ECS device, an analytical mathematical model was developed. This model calculates the forces felt by an operator as a function of the piston geometry, applied voltage and the motion characteristics imposed by the operator. In this section, a summary of the model equations is presented and two cases are distinguished: static and dynamic.

It can be shown that the static reaction force  $F_{R,s}$  is given by:

$$F_{R,s} = NC_s L \left[ \left( 2 + \frac{2q}{\ln\left(\frac{r_o}{r_i}\right)} \right) V - (2Dr + q(r_o + r_i)) E_{ref} \right] \quad (3)$$

where:  $N$  is the number of channels,  $C_s$  is the constant associated with the static yield stress (see Equation (2) ),  $L$  is the channel length,  $q$  is the angular width of channel,  $r_o$  is the outer radius,  $r_i$  is the inner radius,  $Dr$  is the channel width ( $r_o - r_i$ ) (see also Figure 7 where the geometric parameters are defined.),  $V$  is the applied voltage and  $E_{ref}$  is the constant reference field.

The following equation can be developed to express the total dynamic reaction force  $F_{R,d}$ :

$$F_{R,d} = \left( \frac{Nr_o^2}{2} \right) NL \left[ \left( C_d - C_v \frac{v}{Dr} \right) \left( \frac{q}{r_o} + \frac{q}{r_i} + \frac{2}{r_i} - \frac{2}{r_o} \right) \frac{V^2}{\left( \ln\left(\frac{r_o}{r_i}\right) \right)^2} + m_b \left( 2 + q \left( \frac{r_o + r_i}{Dr} \right) \right) v \right] - rL \left( Nr_o^2 - \frac{Nq}{2} (r_o^2 - r_i^2) \right) a \quad (4)$$

where the additional variables are:  $C_d$ , the constant associated with dynamic yield stress;  $C_v$ , the constant associated with viscosity;  $v$ , the velocity;  $m_b$ , the dynamic viscosity with no electric field applied;  $r$  the density;  $a$ , the acceleration.

In Equation (4), the total reaction force is the sum of four terms: a) a term proportional to the square of the voltage applied; b) a term proportional to the velocity; c) a term proportional to the acceleration; d) a term proportional to the product of the velocity and the square of the voltage.

### 4. DESIGN OF THE ECS ELEMENTS

The analytical equations developed in Section 3, will be used to evaluate the effects on the reaction forces felt by the user when various geometric and input parameters are changing. The results from this study are very important for the design of the ECS elements.

Human studies have shown that the controllable maximum force that a human finger can exert is between 40 and 50 N [3]. However, maximum exertion forces create discomfort and fatigue to the human operator. Comfortable values of exertion forces are between 15 to 25% of the controllable maximum force exerted by a human finger. Hence, the design objective is to develop an ECS element that will be able to apply a maximum force of 15N to the operator. We are primarily interested in the dependence of the reaction forces from the ECS when the following parameters are changing: voltage applied  $V$ , motion characteristics imposed by the user such as the velocity  $v$ , and acceleration  $a$ , and geometric characteristics of the piston such as geometry of the channel defined by the inner and outer diameters  $r_i$  and  $r_o$ , and the angle of the channel  $q$ . Therefore in our study, it is desired to find out the ranges of values for these parameters that will result in the desired maximum force output of 15N.

This parametric analysis will be performed for the dynamic case because as the ECS element will be used to mirror remote or virtual compliance, always it will be in motion. In static cases such as when remote or virtual contact forces and weight have to be reflected, the MEMICA system will be equipped with a different type of elements called force feedback actuation tendon (FEAT) elements, which would employ other type of actuators. Hence, Equation (4) is used to calculate the reaction forces. Certain default values have been selected for the parameters used in Equation (4). The parameters related to the fluid ERF LID 3354 have been determined from the manufacturer's specifications [29] and are shown in Table 1. The default geometric parameters of the ECS element, that are shown in Table 2, have been determined from the dimensions of commercially available sensors and electronic equipment that will be used for measuring and actuating the device and also by manufacturing and machinability constraints. In the first prototype, that is presented in this work (see Section 6), no effort for miniaturization was made since the goal was to prove the concept that ERFs can be used to create haptic feedback. The default values for motion characteristics were selected based on the maximum velocities and accelerations that a human finger can develop.

**Table 1.** ERF LID 3354 Parameters

$C_d$	0.00026
$C_v$	0.198 E-7
$m_b$	0.125
$r$	1460kg/m <sup>3</sup>

**Table 2.** Defaults Values for the Geometric Parameters

$L$	0.0254m
$r_i$	0.011316m
$r_o$	0.012065m
$Dr$	0.000749m
$N$	12
$q$	0.47 rad (27°)

**Table 3.** Defaults Values for the Motion Characteristics

$a$	0.01m/s <sup>2</sup>
$v$	0.1m/s

#### 4.1 Contribution of the Applied Voltage

Voltage is the principal parameter of interest in this study since it will be used for controlling the compliance of the ERF. It is desired to calculate the maximum voltage that is needed for achieving a reaction force of 15N. Setting the default values in Equation (4) and changing the voltage from 0 to 1kV the force has been calculated and is shown in Figure 8. As expected the relationship of the force to the voltage is parabolic. A voltage of 1kV will be needed to generate the required force. The need of high voltage using the ERF's was expected. However, as it is demonstrated in Section 6, a low power circuit has been developed to generate the high voltage with a very low current.

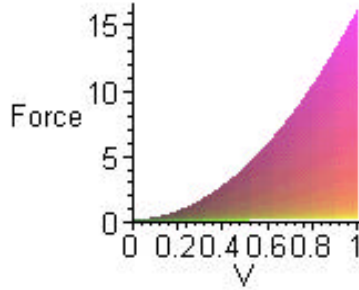


**Figure 8.** Dynamic Force (N) as a Function of Voltage V (kVolts)

#### 4.2 Contribution of the Velocity and Acceleration

The velocity  $v$  of the piston with respect to the interior of the cylinder is changing from 0 to 0.5m/s while the voltage is changing from 0 to 1kV. The calculated force is shown in Figure 9. It is clearly seen that the reaction force is almost independent of the velocity. This is due to the velocity contribution in the reaction force is much smaller than the effect of the voltage related term. For the same reason, the acceleration does not affect the total reaction that is felt by the human operator.

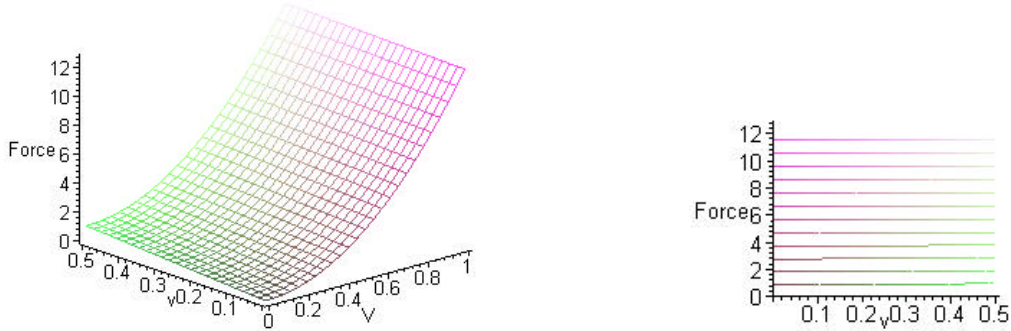


**Figure 9.** Force (N) as a Function of Velocity  $v$  (m/s) and Voltage V (kVolts)

#### 4.3 Contribution of the Geometric Parameters

The outer diameter of the piston changes from 0.012m to 0.014m while the voltage changes from 0 to 1kV. All other parameters take the default values shown in Tables 1, 2 and 3. The calculated reaction forces are shown in Figure 10. It is clearly seen that as the outer diameter increases the reaction force decreases dramatically. On the other hand as the outer diameter approaches the value for the channel inner diameter the reaction forces take infinite values. This shows that the thinner the piston channels the larger the reaction force is and hence the required voltage can be reduced. However, mechanical limits such as the precision of the tools used and the machinability of the material impose a practical limit on the value for the channel thickness.

In a similar way, the channel angle changed from 0 to 0.5 radians and the force was calculated (see Figure 11). Under a certain minimum value of  $q$ , the reaction force drops dramatically (Figure 11). In this case, the pressure force becomes too great with respect to the shear force induced by the applied electric field. Also there is a maximum limit for  $q$  after which the reaction force is constant. Therefore optimal values for  $q$  are around 0.4 radians (i.e. 30 degrees).

The parameters  $N$  and  $L$  affect in a linear way the reaction force. Increasing these parameters increases the force for a given voltage. However, the dimensions of the piston limit  $L$  and the number of channels  $N$  is limited by the values of  $q$ .



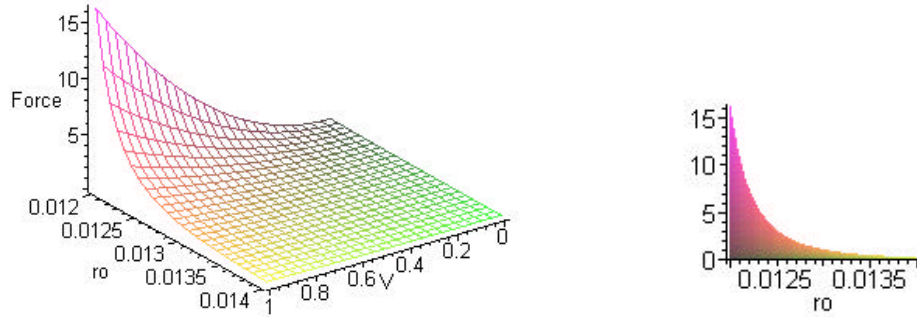


**Figure 10.** Force (N) as a Function of the Outer Diameter  $r_0$  (m) and Voltage  $V$  (kVolts)

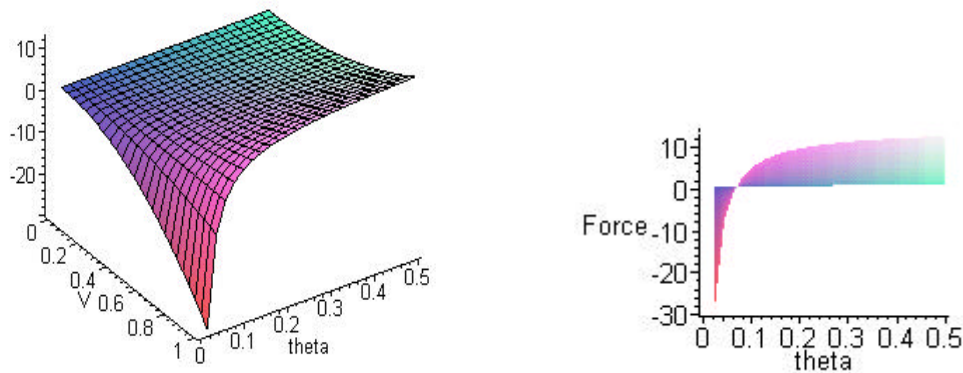


**Figure 11.** Force (N) as a Function of Voltage (kVolts) and Channel Angle  $q$  (radians)

## 5. EXPERIMENTAL SYSTEM

In order to test the concept of controlling the stiffness with a miniature ECS element, a larger scale test-bed has been built at the Rutgers Robotics and Mechatronics Laboratory. This test-bed, that is shown in Figures 12 and 13, is equipped with temperature, pressure, force and displacement sensors that will be used for monitoring the ERF's state. The support structure of the testbed is constructed with aluminum to decrease overall weight. The cylinder, however, is mounted on a fixed stainless steel plate to maintain rigidity during normal force loading. The top plate is also stainless steel and serves as the base for the weight platform. Though a linear actuator can be used to apply forces axially to the cylinder, this system simply employs calibrated brass weights. The weight platform referenced in Figure 12 is where the weights are to be placed for testing. Beneath the platform around the stainless steel shaft is a quick release collar, which allows the force to be released by the operator. The shaft, which transmits the force down into the cylinder, is restrained to only one-dimensional motion through the linear bearing mounted to the top plate. The  $\frac{1}{2}$  inch solid shaft is reduced by an adapter to a  $\frac{1}{4}$  inch aircraft steel hollow shaft. At this junction there is a load cell and flange bracket mounted for the wiper shaft of the displacement sensor. The  $\frac{1}{4}$  inch shaft inserts through the ERF chamber's top plate and a small bundt cup needed to minimize leaking from the chamber during operation. Within the chamber the experimental piston is attached to the shaft with e-clips secured at the top and bottom of the piston. The chamber itself is a one-inch internal diameter beaded Pyrex piping sleeve, which is six inches in length. Using Pyrex allows for visual observation of the ERF during actuation. In order to apply voltage to the fluid, the supply wires are run down through the hollow shaft and into the piston, where the electrical connections are made to the channel plates. Threaded into the bottom plate of the chamber is the dual pressure and temperature sensor. The final sensor is mounted along side the chamber and affixed with a flanged bracket from the chamber.

There are six system parameters that are measured during experimentation: voltage, current, force, displacement, pressure and temperature. All sensor signals are interfaced directly to Analog-to-Digital boards located in a Pentium II PC and are processed using the Rutgers WinRec v.1 real time control and data acquisition Windows NT based software. In addition, all sensors are connected to digital meters located in the interface and control box. For the sensors, excitation voltages are supplied by five volts from the PC or by the meter provided with the sensor itself. The ERF power system is a small supply circuit originally designed for night vision scopes [30]. This power supply is capable of producing 4.5-KV from a standard 9-V battery. By modifying this circuit to produce a PC adjustable straight DC voltage, linear control of the viscosity is

implemented with programmed software control. This power system allows for portability in later prototypes. All the interface and control circuitry are housed in a portable ventilated enclosure.

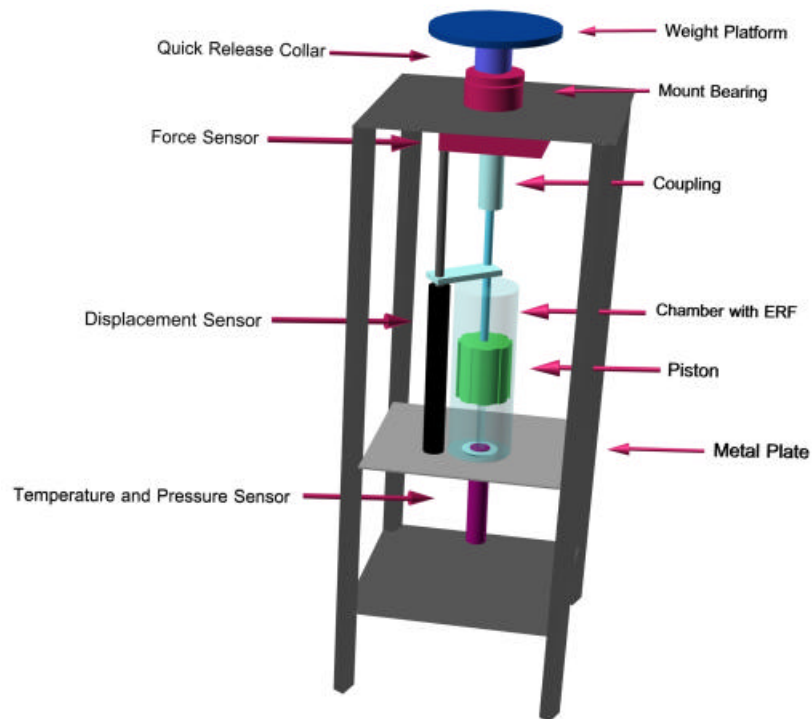


**Figure 12.** Experimental Test-bed

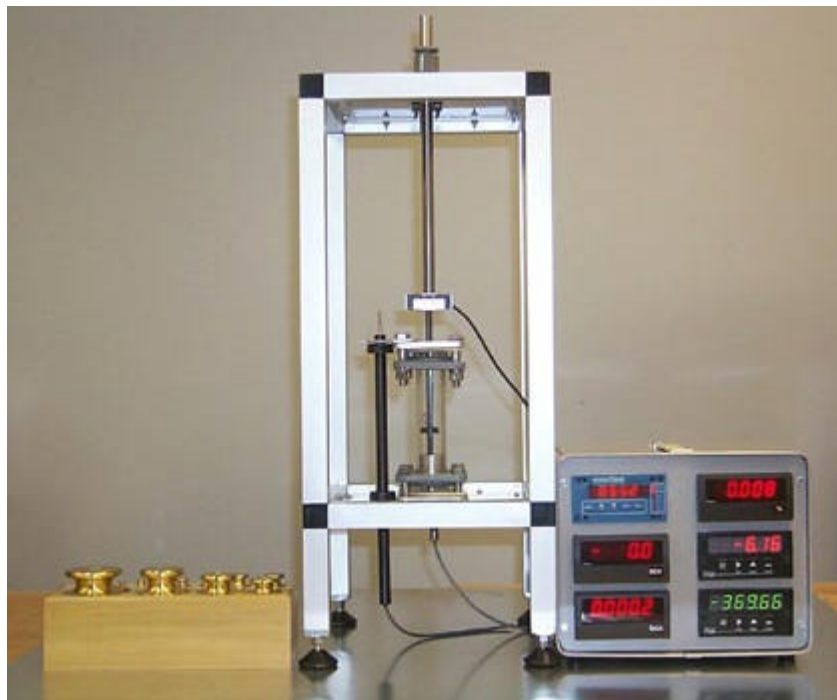


**Figure 13.** Actual Prototype System

## 6. CONCLUSIONS

For many years, the robotic community sought to develop robots that can eventually operate autonomously and eliminate the need for human operators. However, there is an increasing realization that there are some tasks that humans can perform significantly better but, due to associated hazards, distance, physical limitations and other causes, only robots can be employed to perform these tasks. Remotely performing these tasks by operating robots as human surrogates, which is referred to as telepresence, requires an intuitive way to allow the operator to feel like physically being present at the remote site. Haptic feedback is necessary to mirror the stiffness and forces to the human operator from the remote site, which can be virtual.

Using electroactive polymers or smart materials can enable to develop many interesting devices and methodologies to support the need for haptic interface in such areas as automation, robotics, medical, games, sport and others. The authors studied the use of Electrorheological fluids to allow "feeling" the environment at remote or virtual robotic manipulators. A new device was introduced for operators to sense the interaction of forces exerted upon a robotic manipulator that is being controlled. An analytical model was developed and experiments were conducted on the so-called electrically controlled stiffness (ECS) element, which is the key to the new haptic interface. A scaled size experimental unit was constructed and allowed to demonstrate the feasibility of the mechanism.

## 7. ACKNOWLEDGEMENTS

This work was supported by NASA's Jet Propulsion Laboratory and CAIP - the Center for Computer Aids for Industrial Productivity. Mr. Alex Paljic, Mr. James Celestino, Mrs. Jamie Lennon and Mrs. Sandy Larios provided important assistance during the development of this work.

## 8. REFERENCES

1. Sheridan T., 1992, *Telerobotics, Automation, and Human Supervisory Control*, MIT Press, Cambridge, MA.
2. Papper M. and Gigante M., 1993, "Using Physical Constraints in a Virtual Environment," in *Virtual Reality Systems*, Academic Press, Orlando, FL, pp.107-118.
3. Burdea, G., 1996, *Force and Touch Feedback for Virtual Reality*, New York: John Wiley and Sons.
4. Johnson Space Center, 1997, <http://tommy.jsc.nasa.gov/robonaut/Robonaut.html> .
5. Lovchik C.S. and Diftler M.A., 1999, "The Robonaut Hand: A Dexterous Robot Hand for Space", *Proceedings of the 1999 IEEE International Conference on Robotics and Automation*, Detroit, MI.
6. Li, L. 1993, "Virtual Reality and Telepresence Applications in Space Robotics," *Virtual Reality Systems*, Vol. 1, No. 2, pp. 50-56.
7. Burdea G. and N. Langrana, 1993, "Virtual Force Feedback: Lessons, Challenges, Future Applications," *Journal of Robotics and Mechatronics*, Vol. 5, No. 2, Japan.
8. Cybernet Systems Co., 1995, Company brochure, Ann Arbor, MI.
9. Immersion Corp., 1999, <http://www.force-feedback.com/research/research.html>.
10. Haptic Technologies, 1999, <http://www.haptech.com/prod/index.htm>.
11. Massie T. and K. Salisbury, 1994, "The PHANToM Haptic Interface: A Device for Probing Virtual Objects," *ASME Winter Annual Meeting*, DSC-Vol. 55-1, pp. 295--300.
12. Sensable Technologies, 1999, <http://www.sensable.com/products/desktop.htm>
13. Luecke G., 1995, "Robotic & Magnetic interface for Force Interaction with Virtual Reality," National Science Foundation Grant, Robotics and Machine Intelligence, Washington DC.
14. Bejczy, A., and J. Salisbury, 1980, "Kinematic Coupling Between Operator and Remote Manipulator," *Advances in Computer Technology*, Vol. 1, pp. 197--211, ASME.
15. Jau, B., A. Lewis and A. Bejczy, 1994, "Anthropomorphic Telematuration in Terminus Control Mode," *Proceedings of Ro-ManSy'94*.
16. Burdea G., J. Zhuang, E. Roskos, D. Silver and N. Langrana, 1992, "A Portable Dexterous Master with Force Feedback," *Presence -- Teleoperators and Virtual Environments*, Vol. 1(1), pp. 18--28.

17. Gomez D., G. Burdea and N. Langrana (1995), "Integration of the Rutgers Master II in a Virtual Reality Simulation," *IEEE Virtual Reality Annual International Symposium (VRAIS)*, pp. 198--202.
18. Virtual Technologies, 1999, <http://www.virtex.com/>
19. Bar-Cohen Y., Mavroidis, C., Pfeiffer C., Culbert C. and Magruder D., 1999, "Haptic Interfaces", Invited Chapter in *Automation, Miniature Robotics and Sensors for Non-Destructive Testing and Evaluation*, Y. Bar-Cohen Editor, April 99.
20. Bar-Cohen Y., Pfeiffer C., Mavroidis C. and Dolgin B., 1999, "MEMICA: A Concept for Reflecting Remote-Manipulator Forces", NASA Technical Briefs.
21. Winslow, W. M., 1949, "Induced Fibrillation of Suspensions," *Journal of Applied Physics*, Vol. 20, pp. 1137.
22. Block, H. and Kelly, J. P., 1988, "Electro-Rheology", *Journal of Physics, D: Applied Physics*, Vol. 21, pp. 1661.
23. Gast, A. P., and Zukoski, C. F., 1989, "Electrorheological Suspensions as Colloidal Suspensions," *Advances in Colloid and Interface Science*, Vol. 30, pp. 153.
24. Duclos, T., Carlson, J., Chrzan, M. and Coulter, J. P., 1992, "Electrorheological Fluids – Materials and Applications," in *Intelligent Structural Systems*, Tzou and Anderson (editors), Kluwer Academic Publishers, pp. 213-241, Netherlands.
25. Bullough, W. A., Johnson, A. R., Hosseini-Sianaki, A., Makin, J. and Firoozian, R., 1993, "Electro-Rheological Clutch: Design, Performance Characteristics and Operation," *Proceedings of the Institution of Mechanical Engineers, Part I, Journal of Systems and Control Engineering*, Vol. 207, No. 2, pp. 87-95.
26. Choi, S. B., 1999. "Vibration Control of a Flexible Structure Using ER Dampers," *Transactions of the ASME, Journal of Dynamic Systems, Measurement and Control*, Vol. 121, pp. 134-138.
27. Stanway, R., Sproston, J. L., and El-Wahed, A. K., 1996, "Applications of Electro-Rheological Fluids in Vibration Control: A Survey," *Smart Materials and Structures*, Vol. 5, No. 4, pp. 464-482.
28. Furusho J., Zhang G. and Sakaguchi M., 1997, "Vibration Suppression Control of Robot Arms Using a Homogeneous-Type Electrorheological Fluid," *Proceedings of the 1997 IEEE International Conference on Robotics and Automation*, Albuquerque, NM, pp. 3441-3448.
29. ER Fluids Developments Ltd, 1998, "Electro-Rheological Fluid LID 3354," *Technical Information Sheet*, United Kingdom.
30. Graf, R. and Sheets, W., 1996, *Encyclopedia of Electronic Circuits*, Volume 6, McGraw-Hill.